THE CORROSION BEHAVIOR OF CHROMIUM NITRIDE FILM ON AISI 4140 AND H13 STEELS

Pornwasa Wongpanya[1*], Thipusa Wongpinij[2], Pat Photongkam[2], Chonthicha Keawhan[2], Sarayut Tunmee[3], and Nirun Witit-Anun[4]

Received: June 18, 2015; Revised date: September 22, 2015; Accepted date: September 22, 2015

Abstract

Chromium nitride film (CrN) was prepared on steel substrates, AISI 4140 and H13 with variations in the substrate roughness, using the reactive DC magnetron sputtering technique at room temperature in controlled partial pressures of Ar and N_2 gas atmospheres. The films were polycrystalline, as confirmed by X-ray diffraction analysis. The corrosion behavior was investigated using an electrochemical technique in 3.5 wt% NaCl solution with various pH values at room temperature. The results indicated that the CrN-coated AISI H13 presents better corrosion resistance than the CrN-coated AISI 4140 at pH 2 and 7, but worse at pH 10. In addition, the rate of corrosion decreased with a reduction of the surface roughness. The chemical states of the corrosion product were clearly identified by spatially resolved secondary electron yield X-ray absorption spectroscopy with X-ray photoemission electron microscopy. It was found that Cr_2O_3 is formed on the non-corroded CrN film and the AISI H13 substrate, whereas Fe_2O_3 is formed on the corroded surface and the AISI 4140 substrate.

Keywords: Chromium nitride, corrosion behavior, electrochemical technique, X-ray photoemission electron microscopy, X-PEEM

Introduction

Metal-nitride films are extensively employed as a protection film for surface improvement of engineering parts. They not only represent high hardness and high wear resistance, but they also protect the substrate from corrosion in liquid environments (Zhou *et al*., 2003: Merl *et al*., 2004). Chromium nitride (CrN) is inexpensive compared with other nitrides, such as titanium nitride, titanium aluminium nitride, and titanium aluminium silicon nitride, and its performance in terms of corrosion and wear resistance is generally utilized for many applications, e.g.

[1] *School of Metallurgical Engineering, Institute of Engineering, Suranaree Universit y of Technology, Nakhon Ratchasima, 30000, Thailand. Tel. 0-4422-4486; Fax. 0-4422-4482; E-mail: pornwasa@sut.ac.th*

[2] *Synchrotron Light Research Institute (Public Organization), Nakhon Ratchasima, 30000, Thailand.*

[3] *Department of Materials Science and Technology, Nagaoka University of Technology, 16031-1 Kamitomioka-machi 940-2188, Japan.*

[4] *Department of Physics, Faculty of Sciences, Burapha University, Chonburi, 20131, Thailand.*

[*] *Corresponding author*

auto mobile parts, cutting tools, and molds. Many researchers (Keawhan *et al*., 2012; Wongpanya *et al*., 2014) have demonstrated that CrN-coated steels with a difference in the substrate roughness significantly improved their corrosion resistance. They reported that the CrN-coated steels exhibited better corrosion resistance than the uncoated steels and the corrosion rate can be reduced by decreasing the roughness of the steel substrate. In addition, the corrosion behavior of CrN-coated steels drastically changed with the pH of the solution, in particular for an acid solution (Trépanier and Pelton, 2005). However, there still remains a question about how the type of steel substrate affects the corrosion behavior of the CrN film. In this paper, the focus was on the evaluation of the corrosion resistance of the CrN coating on AISI 4140 and H13 steels. The corrosion resistance of the CrN-coated and uncoated steels in 3.5 wt% sodium chloride (NaCl) solution was tested by an electrochemical method. Since some engineering parts were used in liquid environments, they were used in contact with both acid and alkaline solutions. Therefore, corrosion was tested in the solution at pH 2, 7, and 10 which is a more realistic approach towards solving the problem of metal corrosion. After the electrochemical testing, the corroded surfaces of the CrN-coated and uncoated steels were investigated by scanning electron microscopy (SEM), and X-ray photoemission electron microscopy (X-PEEM) was used to evaluate the corrosion products on the corroded surfaces of the CrN-coated steels.

Materials and Methods

Sample Preparation

First, samples of AISI 4140 and H13 steels were prepared with dimensions of 10×10×2 mm^3. The chemical compositions investigated by atomic emission spectroscopy are shown in Table 1. The samples were heated for 30 min at 850°C (AISI 4140) and 1025°C (AISI H13); subsequently they were oil–quenched and tempered. The samples were polished with silicon carbide (SiC) paper at various grit numbers, e.g. 180, 600, and 1200 to prepare the different substrate roughnesses. The microstructures of these steels were studied by light optical microscopy. The samples were ground, polished, and etched for metallographic microstructure evaluations. An etchant solution used to reveal the microstructure was prepared from a 2% nital solution composed of 2 ml nitric acid and 98 ml ethyl alcohol. The microstructure of the AISI 4140 steel was found to consist of a mixture of ferrite and pearlite, whereas the microstructure of the AISI H13 steel was composed of ferrite and carbide in the normalizing condition, as shown in Figure 1(a) and 1(b). After heat treatment, the microstructure of the AISI 4140 and H13 steels had changed to martensite and retained austenite, as shown in Figure 1(c) and 1(d). Before coating with CrN, the substrate samples were rinsed with distilled water and acetone and were air-dried. The DC magnetron sputtering process was employed to deposit the CrN film on these samples with the deposition conditions shown in Table 2. A list of the samples for the corrosion evaluation dependent on the steel types and surface roughness is shown in Table 3.

Corrosion Testing

The corrosion behavior of the uncoated and CrN-coated samples was evaluated by an electrochemical technique in accordance with ASTM standard G44-99 (ASTM, 2005). Experiments were performed using a potentiostat analyzer; an electrochemical cell contains 3 electrode cells including the samples

Table 1. Chemical composition of AISI 4140 and H13 steels (in wt%) determined by atomic emission spectroscopy

Grade	C	Cr	Si	Mn	Mo	V	Fe
AISI 4140	0.47	0.81	0.26	0.78	0.19	-	Bal.
AISI H13	0.42	5.40	0.48	0.35	1.12	0.81	Bal.

as a working electrode, graphite as a counter electrode, and silver/silver chloride (Ag/AgCl with 3.0 M KCl) as a reference electrode. The samples were polarized to a potential between -900 mV and +200 mV at a scan rate of 1.0 mV/s in 3.5 wt% NaCl solution with pH values of 2, 7, and 10 at room temperature. The pH of the solution was adjusted by the addition of hydrochloric acid (HCl) and sodium hydroxide (NaOH). The polarization curves were used to study the corrosion behavior of the samples. The study was carried out in order to obtain the

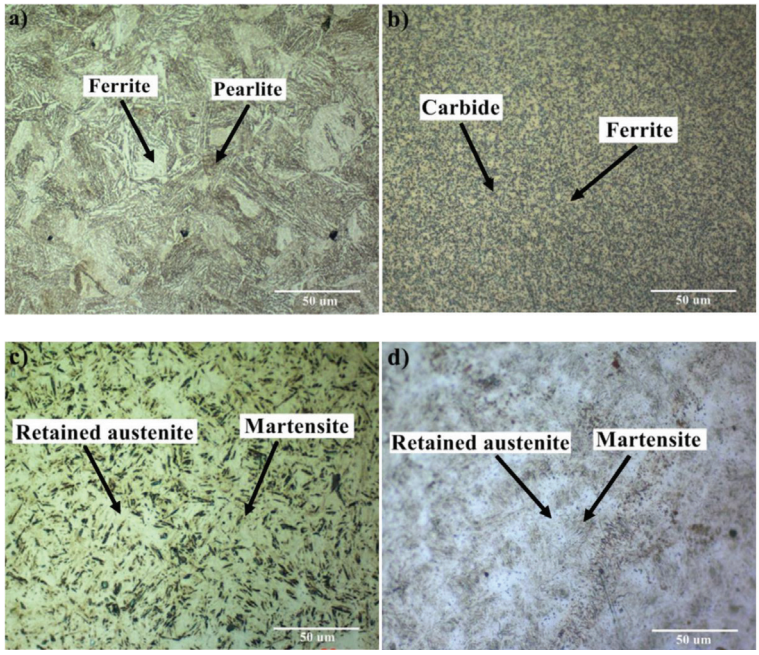

Figure 1. Microstructures of the substrate samples; a) AISI 4140, b) AISI H13, c) AISI4140 after heat treatment, and d) AISI H13 after heat treatment

Table 2. The deposition conditions of the CrN coating (Keawhan *et al*., 2012; Wongpanya *et al*., 2014)

Ar flow rate (sccm)	6
N_2 flow rate (sccm)	9
Base pressure (mbar)	5.0×10^{-5}
Working pressure (mbar)	3.5×10^{-3}
Ar pressure (mbar)	3.3×10^{-3}
N_2 pressure (mbar)	5.7×10^{-4}
Current (A)	800
Voltage (V)	-456
Deposition time (min)	45
Target-to-substrate spacing (cm)	15
Coating thickness (nm)	914

important corrosion parameters, e.g. corrosion potential (E_{corr}) and corrosion current density (I_{corr}). The corrosion rate (CR) was calculated from the polarization curves according to Faraday's law and was evaluated by the Tafel extrapolation technique.

Structural and Surface Characterizations

The crystallographic phase structure of the CrN films before corrosion testing was studied by X-ray diffraction (XRD). After testing, the corroded surfaces were characterized by SEM and X-PEEM.

Results and Discussions

The Crystallographic Structure of the CrN Film

Figure 2 shows the XRD pattern of the CrN film deposited on the AISI 4140 and H13 steels. The XRD analysis reveals that the films deposited on both substrates were polycrystalline with 4 diffraction peaks of CrN (111), (200), (220), and (311) planes at 2θ angles of 37.38º, 43.50º, 63.20º, and 76.20º, respectively. The dominant orientation of the CrN film in this study is the (111) plane. The strong orientation in the (111) plane is also reported by Ruden *et al*. (2013).

Corrosion Behavior

A Comparative Study of the Corrosion Resistance of the Uncoated and CrN-Coated Samples

Figure 3 shows examples of the polarization curves of the AISI 4140-180, AISI H13-180, CrN/4140-180, CrN/4140-1,200, CrN/H13-180, and CrN/H13-1,200 samples tested in 3.5 wt% NaCl solutions at pH 2, 7, and

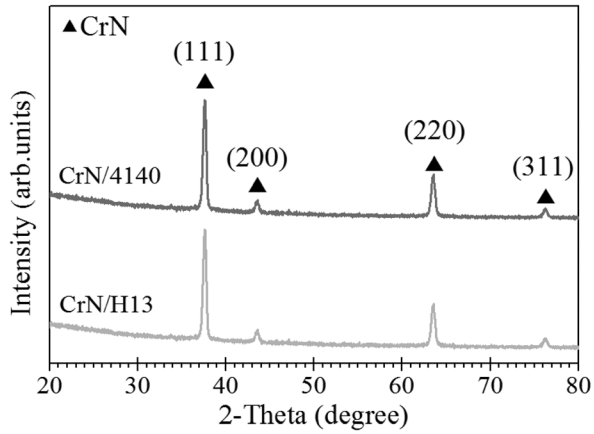

Figure 2. X-ray diffraction pattern of the CrN film on AISI 4140 and H13 steels

Table 3. List of samples for corrosion test

Substrate	SiC paper	Uncoated samples	CrN-coated samples
AISI 4140	No. 180	AISI 4140 - 180	CrN/4140-180
	No. 600	AISI 4140 - 600	CrN/4140-600
	No. 1200	AISI 4140 - 1200	CrN/4140-1200
AISI H13	No. 180	AISI H13-180	CrN/H13-180
	No. 600	AISI H13-600	CrN/H13-600
	No. 1200	AISI H13-1200	CrN/H13-1200

10. In Table 4, the corrosion parameters of each sample were evaluated from the polarization curves and based on the Tafel equation (Uhlig, 1971). It is obvious that the CrN film highly impacts on the corrosion properties of the AISI 4140 and H13 steels, in particular the corrosion potential (E_{corr}) and corrosion current density (I_{corr}). From a comparison of the E_{corr} of the CrN-coated samples and uncoated samples, it was found that the CrN-coated samples had higher E_{corr} than the uncoated samples. In addition, it was found that the CrN-coated samples showed lower I_{corr} than the uncoated samples (Cunha *et al*., 1999). Thus, the CR of the CrN-coated samples is lower than that of the uncoated samples for all the substrates and pH solutions, as shown in Figure 4. This implies that the corrosion resistance is better with the CrN coated on the surface of the substrates (Liu *et al*., 1995; Walter and Mathan, 2011). Those results indicated that CrN-coated samples have a better corrosion resistance than that of the uncoated samples. The corrosion resistance of the CrN-coated samples is attributed to the presence of chromium (Cr) and nitrogen (N) atoms within the CrN film. After the CrN film reacted with the corrosive solution, the chromium atoms were oxidized to chromium oxide. It is well known that chromium oxide is a stable oxide film and it is able to inhibit corrosion (Ibrahim *et al*., 2002; Lippitz and Hubert, 2005; William Grips *et al*., 2006). The nitrogen atoms in the CrN film are dissolved into the solution in the form of nitrogen anions (N^-) during corrosion, and then they repel chloride anions (Cl^-) away from the surface of the samples. Moreover, the nitrogen anions combine with hydrogen ions (H^+) in the solution to form the ammonium (NH_4^+), as shown in Equation (1), which results in the increased pH of the solution. As a result, corrosion attack from the solutions decreases (Chyou and Shih, 1991; Grabke, 1996).

$$N(s)+4H^+(aq)+3e^- \rightarrow NH_4^+(aq) \qquad (1)$$

Effect of Steel Types on Corrosion Behavior

Figure 4 shows the corrosion rate of the uncoated and CrN-coated samples dependent on the steel types. It is obvious that the AISI H13 and CrN/H13 samples show a lower corrosion rate than the AISI 4140 and CrN/4140 samples, respectively, at pH 2 and 7. This might be due to the chemical compositions of the substrate, as shown in Table 1. The AISI H13 steel (5.40%Cr) has a chromium content higher than that of the AISI 4140 steel (0.81%Cr). This means that chromium oxide developed on the surface of the

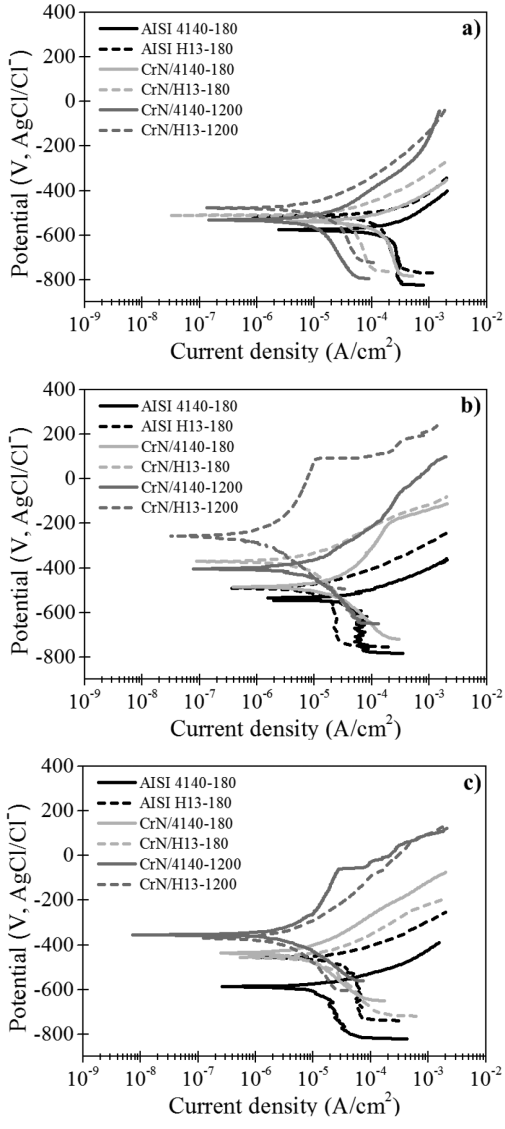

Figure 3. The polarization curves of samples in 3.5 wt% NaCl solution at a) pH 2, b) pH 7, and c) pH 10

Table 4. Corrosion parameters obtained from the polarization curves of the uncoated and CrN-coated samples

pH	Samples	SiC paper	E_{corr} (mV)	I_{corr} ($\mu A/cm^2$)	CR (mm/year)
pH2	AISI 4140	No.180	-571	175.00	1.9356
		No.600	-595	67.00	0.7786
		No.1200	-559	52.00	0.6043
	AISI H13	No.180	-514	120.00	1.3946
		No.600	-578	55.00	0.6392
		No.1200	-473	42.92	0.4992
	CrN/4140	No.180	-538	75.00	0.9382
		No.600	-520	20.00	0.2502
		No.1200	-518	12.50	0.1563
	CrN/H13	No.180	-509	26.00	0.3252
		No.600	-500	18.07	0.2240
		No.1200	-499	7.24	0.0897
pH7	AISI 4140	No.180	-535	32.00	0.3719
		No.600	-535	21.00	0.2440
		No.1200	-598	12.00	0.1394
	AISI H13	No.180	-478	18.17	0.2113
		No.600	-527	7.55	0.0878
		No.1200	-534	4.36	0.0507
	CrN/4140	No.180	-485	16.00	0.2001
		No.600	-442	8.50	0.1063
		No.1200	-400	6.50	0.0813
	CrN/H13	No.180	-361	7.00	0.0875
		No.600	-407	6.18	0.0766
		No.1200	-291	1.33	0.0165
pH10	AISI 4140	No.180	-582	18.00	0.2091
		No.600	-595	12.50	0.1564
		No.1200	-559	7.00	0.0813
	AISI H13	No.180	-450	35.06	0.4078
		No.600	-352	15.25	0.1773
		No.1200	-482	16.05	0.1867
	CrN/4140	No.180	-465	9.00	0.1126
		No.600	-421	4.50	0.0563
		No.1200	-419	2.20	0.0275
	CrN/H13	No.180	-442	14.00	0.1751
		No.600	-389	6.50	0.0813
		No.1200	-386	3.70	0.0460

AISI H13 more easily than on the surface of the AISI 4140. As a result, the AISI H13 and CrN/H13 samples have better corrosion resistance than the AISI 4140 and CrN/4140 samples, respectively.

In contrast, the uncoated AISI 4140 shows a lower corrosion rate than the uncoated AISI H13 at pH 10, as shown in Figure 4. The solution at pH 10 was adjusted by the addition of sodium hydroxide (NaOH) which results in a higher amount of OH^- and Na^+ as shown in Equation (2). The iron (Fe) in the AISI 4140 substrate is dissolved to become Fe^{2+} and the Fe^{2+} further combines with hydroxide ions (OH^-) to form iron (II) hydroxide ($Fe(OH)_2$), as shown in Equation (3).

$$NaOH(s) \rightarrow Na^+(aq) + OH^-(aq) \quad (2)$$

$$2Fe(s) + O_2(g) + 2H_2O(l) \rightarrow 2Fe^{2+}(aq) + 4OH^-(aq) \rightarrow 2Fe(OH)_2(s) \quad (3)$$

According to the Pourbaix diagram of iron (Beverskog and Puigdomenech, 1996), at pH 10 and with the potential between -0.6 V and 0.0 V, Fe is dissolved to become $Fe(OH)_2$, Fe_3O_4, and Fe_2O_3. This can confirm that at pH 10, the $Fe(OH)_2$ is easily initiated on the AISI 4140 steel. It is believed that the $Fe(OH)_2$ can prevent corrosion but it is an unstable film; also, it can be oxidized to become an iron oxide (Fe_2O_3). Because the AISI H13 steel has chromium oxide, it thus inhibits the diffusion of OH^- into the substrate. As a result, the formation of $Fe(OH)_2$ is difficult. With all the above information, it can be concluded that the uncoated AISI 4140 steel has a higher corrosion resistance than the uncoated AISI H13 steel at pH 10. However, the formation of oxide has to be further evaluated by X-PEEM combined with XAS.

Effect of Substrate Roughness on Corrosion Behavior

It is clearly demonstrated that the roughness of the substrate affects the corrosion rate, as shown in Figure 4. The samples prepared with the greater surface roughness (XX-180 and XX-600) have a higher CR than the samples prepared with the finer surface (XX-1200) for all the pH solutions. This is due to the fact that a rough surface leads to more defects in the CrN film and also results in the samples having

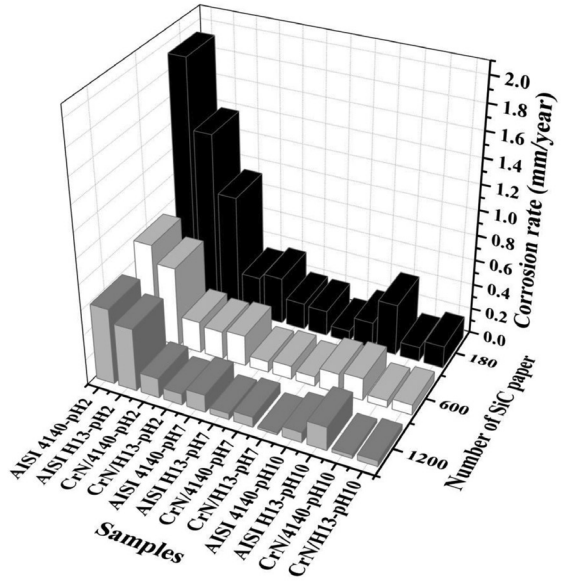

Figure 4. Comparative corrosion rate of the uncoated and CrN-coated samples

a coating with a less complete coverage. Figure 5 shows example images of the surfaces scanned by SEM for the CrN/4140-180, CrN/4140-600, and CrN/4140-1200 samples before the corrosion test; it shows that the CrN/4140-180 sample has more defects than the CrN/4140-600 and CrN/4140-1200 samples, respectively.

Effect of pH of Solution on Corrosion Behavior

It is obvious that the corrosion rate decreases as the pH of the solution increases, as shown in Figure 4. The highest corrosion rate is observed at pH 2 because of the addition of HCl. The Cl^- ions are adsorbed at the surface of the CrN-coated and uncoated samples, then they penetrate and attack the samples, especially at the defects of the CrN film such as the porosity (Hui *et al*., 2003; Mazhar *et al*., 2001). In addition, the high concentration of the hydrogen (H^+) ions in the solution at pH 2 promotes hydrogen evolution causing a higher corrosion rate (Keawhan *et al*., 2012).

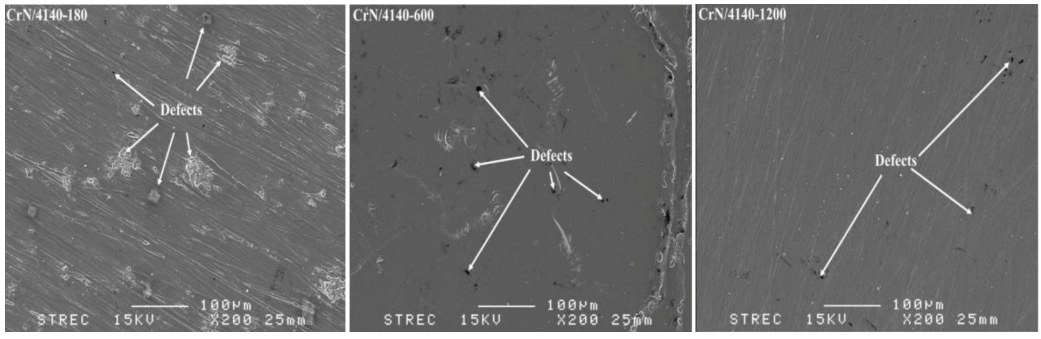

Figure 5. Secondary electron images of the surface of the CrN/4140-180, CrN/4140-600, and CrN/4140-1200 samples before the corrosion test

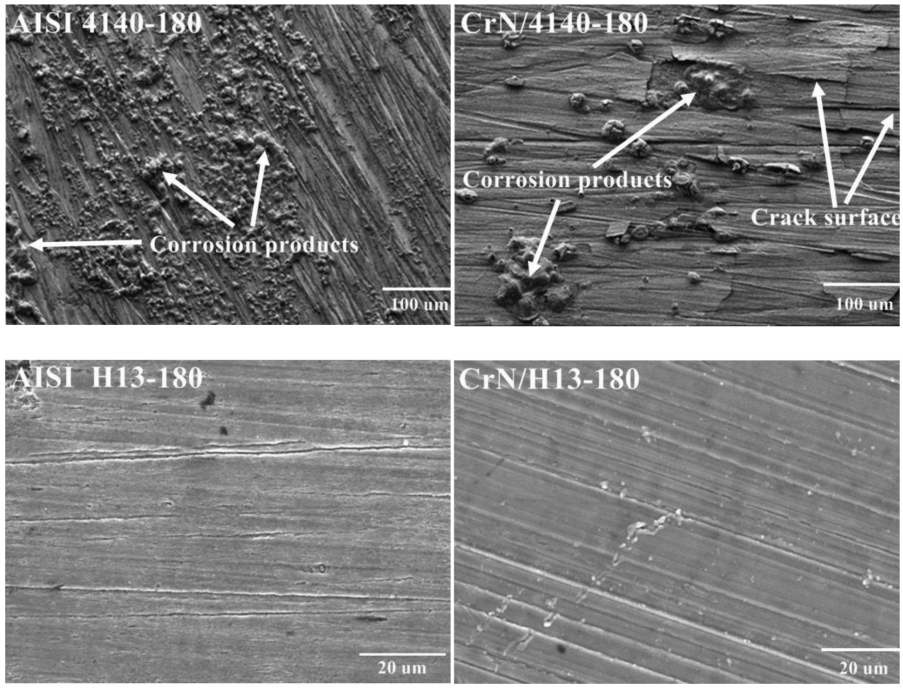

Figure 6. Secondary electron images of the uncoated (AISI 4140-180 and AISI H13-180) and CrN-coated (CrN/4140-180 and CrN/H13-180) samples after the corrosion test in 3.5 wt% NaCl solution

At pH 7 and 10, the hydroxide ions (OH^-) in the solution can react to iron in the substrate to form an unstable hydroxide film which can against corrosion (Beverskog and Puigdomenech, 1996). The passive region of the CrN-coated samples is clearly observed in the polarization curves, as shown in Figure 3(b) and 3(c). This is due to the fact that the CrN film reacts with the OH- in the solution at pH 7 and 10; subsequently, chromium hydroxide ($Cr(OH)_2$) is produced which enhances corrosion resistance. The result is that all of the CrN-coated samples show better corrosion resistance at pH 7 and 10 than at pH 2.

Surface Microstructure Analysis

Since the surfaces of the uncoated and CrN-coated samples are attacked and destroyed by an aggressive solution, corrosion products have been generated. Certain corrosion products, especially oxide formation, were analyzed with SEM and X-PEEM in order to evaluate which

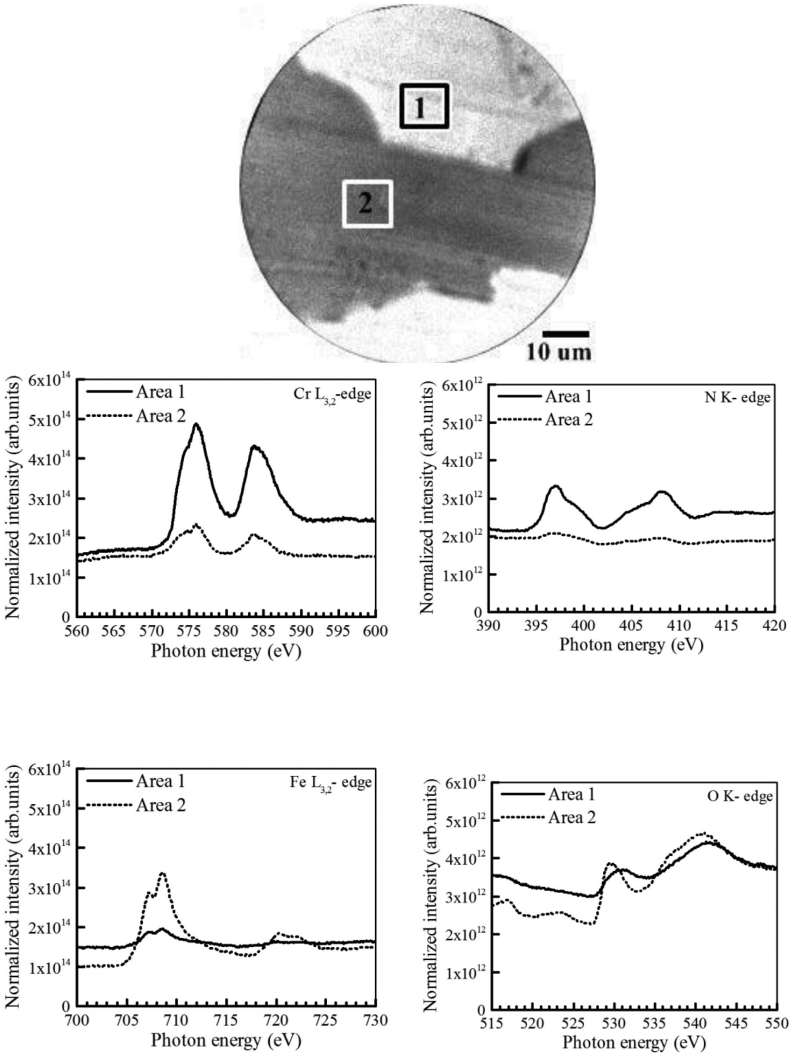

Figure 7. X-PEEM images and XAS spectra of the CrN/H13-180 sample after the corrosion test in 3.5 wt% NaCl solution at pH 2

element or compound is responsible for the corrosion resistance. In this study, the samples tested in the solution at pH 2 were selected for evaluation because such samples show the highest corrosion rate. Figure 6 shows secondary electron images of the uncoated (AISI 4140 and H13) and CrN-coated (CrN/4140 and CrN/H13) samples after the corrosion test at pH 2. The uncoated samples show more degradation than the CrN-coated samples. In addition, it was found that the CrN/4140 sample shows more surface cracks in the film than the CrN/H13 sample. As a result, the corrosion products on the surfaces of the AISI 4140 and CrN/4140 samples are higher than those of the AISI H13 and CrN/H13 samples, respectively.

To identify the compound which is responsible for the corrosion resistance of the CrN-coated samples, the CrN/H13 and CrN/4140 samples immersed in the solution at pH 2 were selected to be investigated by spatially resolved X-ray absorption spectroscopy using X-PEEM. The X-PEEM technique can visualize the surface corrosion and the image intensities were relevant to the X-ray absorption coefficient. These help to characterize the surface by the shapes and sizes of the corroded area. Figure 7 shows the X-PEEM images and XAS spectra of the CrN/H13 sample, with 2 areas, i.e., area 1 with an intact CrN film (Cr- and N-enrichment), and area 2 with the CrN film removed which is deep down in the AISI H13 substrate (Fe-enrichment). The 4 elements, i.e., Cr, N, Fe, and O were investigated at the photon energy of 560 - 600 eV, 390 - 420 eV, 700 - 730 eV, and 515 – 550 eV for the Cr $L_{3,2}$-edge, N *K*-edge, Fe $L_{3,2}$-edge, and O *K*-edge, respectively (Guiot *et al*., 1999; Frazer *et al*., 2003; Hocking *et al*., 2006; Wasinger *et al*., 2003; Esaka *et al*., 1997; Schedel-Niedrig, 1998). These 4 elements were evaluated since Cr and N are the main components of CrN film while Fe is a main component of the AISI H13 substrate and O is a main component of the oxide generated as a result of the corrosion reaction. It is obvious that the CrN film (area 1) showed a high intensity of the Cr $L_{3,2}$-edge, and N *K*-edge, while the low intensity of the O K-edge and Fe $L_{3,2}$-edge were detected. At the area with

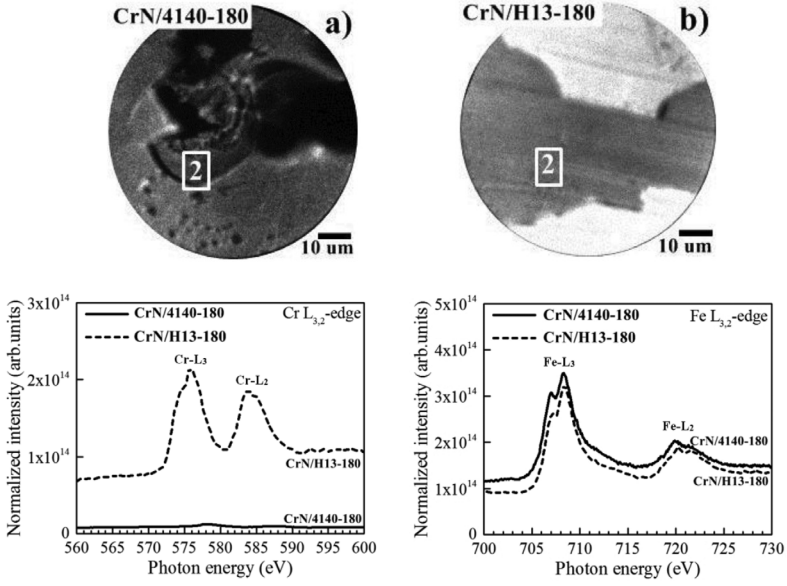

Figure 8. Comparative X-PEEM images and XAS spectra of the CrN/4140-180 and CrN/H13-180 samples after the corrosion test in 3.5 wt% NaCl solution at pH 2

the CrN film removed (area 2), high intensity of the Fe $L_{3,2}$-edge, Cr $L_{3,2}$-edge, and O *K*-edge was shown, while the low intensity of the N *K*-edge was detected. The implication is that Cr had oxidized in both areas. The oxidation of Cr to become chromium oxide (Cr_2O_3) is a vital key for corrosion protection of the CrN film (Schedel-Niedrig, 1998; Cunha *et al*., 1999). The XAS spectrum of the Fe $L_{3,2}$-edge was detected at area 2; this reveals the oxidation of Fe into rust (Fe_2O_3) (Hocking *et al*., 2006). $Fe(OH)_2$ is unstable, so it cannot be detected which confirms that it was transformed into Fe_2O_3.

To study the effect of the substrate steels on the corrosion of the CrN film, X-PEEM images and XAS spectra of the CrN/4140 and CrN/H13 samples after being tested at pH 2 were comparatively evaluated. For area 2, where the CrN film was removed due to the corrosion reaction, 2 samples were analyzed in particular for Cr and Fe, as shown in Figure 8. It is obvious that both samples show the spectra of the Fe $L_{3,2}$-edge, but the CrN/H13 sample shows a lower intensity of the Fe $L_{3,2}$-edge than the CrN/4140 sample. In addition, only the CrN/H13 sample shows the spectra of the Cr $L_{3,2}$-edge. This can be used to confirm that Cr_2O_3 developed at the surface of the AISI H13 substrate. Therefore, the CrN/H13 sample has better corrosion resistance than the CrN/4140 sample. Moreover, it was found that the corroded area of the CrN/4140 sample is deeper than that of the CrN/H13 sample, as shown in Figure 8 a).

Conclusions

The corrosion behavior of the CrN films deposited on the AISI 4140 and H13 substrates was studied. The preferential orientation of the CrN film is in the (111) plane. For the corrosion behavior, the CrN-coated samples exhibited better corrosion resistance than the uncoated samples for all pHs. In addition, it was found that the CrN-coated AISI H13 shows better corrosion resistance than the CrN-coated AISI 4140 for pH 2 and 7. At pH 10, the CrN-coated AISI 4140 has better corrosion resistance than the CrN-coated AISI H13. In addition, the samples prepared with the greater surface roughness have higher corrosion rates than the samples prepared with the finer surfaces. X-PEEM images and XAS measurements have proved to be great techniques to evaluate corroded surfaces and to identify the chemical state of corrosion products. XAS spectra suggest Cr_2O_3 on the CrN film and AISI H13 substrate, and it showed Fe_2O_3 on the corroded surface and AISI 4140 substrate.

Acknowledgements

The authors gratefully acknowledge the financial support for this work by the Office of the National Research Council of Thailand (NRCT), Suranaree University of Technology under Contract No. 61/2553, and Synchrotron Light Research Institute of Thailand (SLRI) under contract No.2552/05. The authors wish to thank the scientists of BL3.2Ub at SLRI for their support during the experiments.

References

ASTM. (2005). Standard practice for exposure of metals and alloys by alternate immersion in neutral 3.5% sodium chloride solution. ASTM: G44-99. ASTM International, West Conshohocken, PA, USA.

Beverskog, B. and Puigdomenech, I. (1996). Revised Pourbaix diagrams for iron at 25°C-300°C. Corros. Sci., 38(12):2121-2135.

Chyou, S.D. and Shih, H.C. (1991). The effect of nitrogen on the corrosion of plasma-nitrided 4140 steel. Corrosion, 1152-1160.

Cunha, L., Andritschky, M., Rebouta, L., and Pischow, K. (1999). Corrosion of CrN TiAlN coatings in chloride-containing atmosphere. Surf. Coat. Tech., 116-119:1149-1150.

Esaka, F., Furuya, K., Shimada, H., Imamura, M., Matsubayashi, N., Sato, T., Nishijima, A., Kikuchi, T., Kawana, A., and Ichimura, H. (1997). XAS study on the intermediate species formed during the surface oxidation of CrN films. J. Phys. IV, 7(C2):1149-1150.

Frazer, B.H., Gilbert, B., Songderegger, B.R., and Stasio, G.D. (2003). The probing depth of total electron yield in the sub-k eV range: TEY-XAS and X-PEEM. Surf. Sci., 537(1-3):161-167.

Grabke, H. J. (1996). The role of nitrogen in the corrosion of iron and steels. ISIJ Int., 36(7):777-786.

Guiot, E., Wu, Z.Y., Gota, S., and Gautier-Soyer, M.

(1999). Polarized O K edge spectra of Fe_2O_3 (0001) nanometric films: A full multiple scattering interpretation. J. Electron Spectrosc., 101-103:3 71-375.

Hocking, R.K., Wasinger, E.C., Groot, F.M.F., Hodgson, K.O., Hedman, B., and Solomon, E.I. (2006). Fe L-Edge XAS studies of $K_4[Fe(CN)_6]$ and $K_3[Fe(CN)_6]$: A direct probe of back-bonding. J. Am. Chem. Soc., 128(32):10442-10451.

Hui, P.F., Cheng, H.H., Jung, K.L., and Yih, H.S. (2003). Effects of PVD sputtered coating on the corrosion resistance of AISI 304 stainless steel. Mater. Sci. Eng., 347(1-2):123-129.

Ibrahim, M.A.M., Korablov, S.F., and Yoshimura, M. (2002). Corrosion of stainless steel coated with TiN, (TiAl)N and CrN in aqueous environments. Corros. Sci., 44(4):815-828.

Keawhan, C., Wongpanya, P., Witit-Anun, N., and Songsiriritthigul, P. (2012). Corrosion behavior of AISI 4140 steel surface coated by physical vapor deposition. Journal of Metals, Materials and Minerals, 22:69-76.

Lippitz, A. and Hubert, T. (2005). XPS investigations of chromium nitride thin films. Surf. Coat. Tech., 200(1-4):250-253.

Liu, C., Leyland, A., Lyon, S.B., and Matthews, A. (1995). An a.c impedance study on PVD-coated mild steel with different surface roughness. Surf. Coat. Tech., 76-77:623-631.

Mazhar, A.A., Arad, S.T., and Noor, E.A. (2001). The role of chloride ions and pH in the corrosion and pitting of Al-Si alloys. J. Appl. Electrochem., 31(10):1131-1140.

Merl, D.K., Panjan, P., Čekada, M., and Maček, M. (2004). The corrosion behavior of Cr-(C, N) PVD hard coatings deposited on various substrates. Electrochim. Acta, 49(9-10):1527-1533.

Ruden, A., Restrepo-Parra, E., Paladines, A.U., and Sequeda, F. (2013). Corrosion resistance of CrN thin films produced by dc magnetron sputtering. Appl. Surf. Sci., 270:150-156.

Schedel-Niedrig, T. (1998). X-Ray absorption spectroscopy: sensitive characterization of (model-) catalysts with the electron yield technique. Fresen. J. Anal. Chem., 361:680-682.

Trépanier, C. and Pelton, A.R. (2005). Effect of temperature and pH on the corrosion resistance of nitinol. Proceedings of the ASM International Materials & Processes for Medical Devices Conference 2004; August 25-27, 2004; Saint Paul, MN, USA, p. 392-397.

Uhlig, H. H. (1971). Corrosion and Corrosion Control. 2nd ed. John Wiley & Sons Inc., Hoboken, NJ, USA, 441p.

Walter, R. and Mathan, B.K. (2011). Influence of surface roughness on the corrosion behavior of magnesium alloy. Mater. Des., 32(4):2350-2354.

Wasinger, E.C., Groot, F.M.F., Hedman, B., Hodgson, K.O., and Solomon, E.I. (2003). L-edge X-ray absorption spectroscopy of non-heme iron sites: experimental determination of differential orbital covalency. J. Am. Chem. Soc., 125(42):12894-12906.

William Grips, V. K., Barshilia, H. C., Selvi, V.E., Kalavati, and Rajam, K.S. (2006). Electrochemical behavior of single layer CrN, TiN, TiAlN caotings and nanolayered TiAlN/CrN multilayer coatings prepared by reactive direct current magnetron sputtering. Thin Solid Films, 514(1-2): 204-211.

Wongpanya, P., Tunmee, S., Euaruksakul, C., Songsiriritthigul, P., and Witit-Anun, N. (2014). Corrosion behavior and mechanical properties of CrN film. Adv. Mat. Res., 853:155-163.

Zhou, Q.G., Bai, X.D., Chen, X.W., Peng, D.Q., Ling, Y.H., and Wang, D.R. (2003). Corrosion resistance of duplex and gradient CrNx coated H13 Steel. Appl. Surf. Sci., 211(1-11):293-299.